



Published in final edited form as:

Neurobiol Dis. 2012 March ; 45(3): 923–929. doi:10.1016/j.nbd.2011.12.011.

DHCEO accumulation is a critical mediator of pathophysiology in a Smith-Lemi-Opitz Syndrome model

Libin Xu, PhD[†], Karoly Mirnics, MD, PhD^{††}, Aaron B. Bowman, PhD[#], Wei Liu, PhD[†], Jennifer Da, Ned Porter, PhD[†], and Zeljka Korade, DVM, PhD^{††,*}

[†]Department of Chemistry and Vanderbilt Institute of Chemical Biology, Vanderbilt University, Nashville, Tennessee 37235

^{††}Department of Psychiatry, Vanderbilt University, Nashville, Tennessee 37235

[#]Department of Neurology, and Vanderbilt Kennedy Center for Research on Human Development, Vanderbilt University, Nashville, Tennessee 37235

Abstract

Smith-Lemli-Opitz syndrome (SLOS) is an inborn error of metabolism caused by defective cholesterol biosynthesis. Mutations within the gene encoding 7-dehydrocholesterol reductase (DHCR7), the last enzyme in the pathway, lead to the accumulation of 7-dehydrocholesterol (7-DHC) in the brain tissue and blood of the SLOS patients. The objective of this study was to determine the consequences of the accumulation of an immediate cholesterol precursor, 7-DHC and its oxysterol metabolite, 3 β ,5 α -dihydroxycholest-7-en-6-one (DHCEO), in the brain tissue of *Dhcr7*-KO mouse, a model for SLOS. We found that cholesterol, 7-DHC and DHCEO show region-specific distribution, suggesting that the midbrain and the cortex are the primary sites of vulnerability. We also report that neurons are ten fold more susceptible to a 7-DHC-derived oxysterol mixture than glial cells, and that DHCEO accelerates differentiation and arborization of cortical neurons. The overall results suggest that 7-DHC oxidative metabolites are critical contributors to altered neural development in SLOS, and that antioxidant supplementation may be extremely valuable for the treatment of this devastating disease.

Keywords

7-dehydrocholesterol; oxysterol; cortical neurons; Smith-Lemli-Opitz Syndrome

INTRODUCTION

Cholesterol is an essential structural component of the central nervous system (CNS). Compared to the rest of the body, the brain contains proportionally the highest amount of cholesterol¹. However, cholesterol shows a highly regional distribution in the CNS, with the highest expression observed in the hippocampus and cortex². Smith-Lemli-Opitz Syndrome (SLOS) is a developmental disorder that arises from mutations in the gene encoding 7-dehydrocholesterol reductase (*DHCR7*), the last step in the cholesterol biosynthesis pathway^{3,4}. The mutation leads to reduced levels of cholesterol, and accumulation of 7-dehydrocholesterol (7-DHC)^{3,4} which is an extremely reactive compound toward free

*Corresponding Author: Zeljka Korade, PhD Department of Psychiatry 8124A MRBIII Vanderbilt University Nashville, TN 37235
Phone: 615-936-1090 Fax: 615-936-3747 zeljka.korade@vanderbilt.edu.

Conflict of Interest

The authors declare no financial interests in relation to the work described.

radical oxidation^{5, 6}. As a result, 7-DHC is oxidized, giving rise to a number of metabolites, namely oxysterols⁶. One of these metabolites, 3 β ,5 α -dihydroxycholest-7-en-6-one (DHCEO)⁷ (Figure 1), shows significant accumulation in fibroblasts of SLOS patients and in the brain of a SLOS mouse model^{7, 8}, raising the possibility that it might significantly contribute to SLOS pathophysiology in the brain of patients.

The regional differences in 7-DHC, DHCEO and their physiological effects on brain development/function are not known to date. To better understand the mechanism by which 7-DHC and its metabolite, DHCEO might contribute to the altered development and brain dysfunction in SLOS, we undertook a series of studies. We determined the distribution of cholesterol, 7-DHC and DHCEO across various brain regions and followed that by assessment of DHCEO effects on neuronal and glial cells.

MATERIALS AND METHODS

Dhcr7-KO Mice – *Dhcr7-KO* (*Dhcr7*^{m1Gst/J}) mice were purchased from Jackson Laboratories (catalogue # 007453). The mice were kept and bred in Division of Animal Care facilities at the Vanderbilt University. For analysis of different brain regions embryos were dissected from pregnant females at E20 and the tail was removed from each embryo for genotyping. The genomic DNA from mouse tails was extracted using REDEExtract-N-Amp Tissue PCR kit (Sigma-Aldrich). Genotyping was performed using the following PCR primers: forward -ggatcttctgagggcagcctt, reverse -tctgaacccttgctgatca, neo: ctgaccgcggctagagaat.

Embryonic heads were removed, brains and specific brain regions dissected and instantly frozen in pre-cooled 2-methylbutane (on dry ice) and stored at -80°C until lipid extraction. All procedures were performed in accordance with the Guide for the Humane Use and Care of Laboratory Animals. The use of mice in this study was approved by the IACUC of the Vanderbilt University.

Primary Neuronal and Astrocytic Cultures

Primary cortical neuronal cultures were prepared from E18 brain tissue as previously described². Briefly, the brain was isolated and the cortex dissected in pre-cooled dissection solution (HBSS). The cortex was cut into tiny pieces and incubated in Trypsin/EDTA for 20-30 min at 37°C. Trypsin was inactivated by adding DMEM medium with 10% FBS (Thermo Scientific HyClone, Logan, UT). Tissue was centrifuged at 80 \times *g* for 5 min and then rinsed with 5 ml of DMEM plus 10% FBS two times. After the second rinse, the tissue was triturated with a fire-polished Pasteur pipette, and the cells pelleted by centrifugation for 5 min at 80 \times *g*. The cell pellet was resuspended in DMEM plus 10% FBS and the cells counted. For determining toxicity of 7-DHC oxysterol mixture the cells were plated on poly-L-lysine coated 96-well plate at density 10⁵/cm² and for testing the effects of DHCEO, the cells were plated on poly-L-lysine coated 24-well plates at density 10⁴/cm². Two hours after plating, the plating medium was completely replaced with Neurobasal medium plus B-27 supplement (Gibco #17504-044) plus L-glutamine plus 5 μ M cytosine arabinoside. To test the effects of DHCEO, 2-3 days after plating, the neuronal medium was completely replaced with either fresh medium or medium plus DHCEO (5 μ M final concentration). After 48 hrs incubation in the cell culture incubator (37°C, 5% CO₂), the cultures were processed for immunocytochemistry.

Primary astrocytic cultures were prepared from P1 brain tissue following the same procedure as for preparation of cortical neurons. After counting, the cells were plated in 60-mm dishes at density 1 \times 10⁶/plate and grown in DMEM medium plus 10% FBS for 10 days. During this time, the astrocytes completely filled the plate. The cultures were extensively

washed with HBSS, trypsinized, resuspended in DMEM plus 10% FBS medium, counted and plated in 96-well plates to determine the toxicity of 7-DHC oxysterol mixture. After 48 hrs, the medium was replaced with fresh medium with or without oxysterol mixture and the astrocytes were incubated in cell culture incubator for additional 48 hrs. The viability of cells was determined using CellTiter 96Aqueous One Solution Cell Proliferation Assay (Promega Corp., Madison, WI) as previously described⁸.

Immunocytochemistry and NeuroLucida[®] At the end of the experiment, the neuronal cultures were washed 2X with phosphate-buffered saline (PBS) and fixed with 4% paraformaldehyde for 15 minutes at room temperature. Following fixation, cultures were washed 3X with PBS and incubated in blocking buffer (PBS with 10% serum and 0.1% saponin) for 30 minutes. The blocking buffer was replaced with primary antibody diluted in the blocking buffer and the cultures were incubated at +4°C overnight. After removing primary antibody solution, the cultures were washed 3X in PBS and then incubated in secondary antibody diluted in blocking buffer for 1 hr at room temperature. After incubation the cultures were washed 3X with PBS. The PBS was completely removed and tiny droplet of Fluoromount was added to each well in 24-well plate. The round 12 mm glass coverslip was gently placed on the top of the cultures. The primary antibodies used in this study are: Tu-20 (mouse monoclonal to neuron specific beta III tubulin, Abcam #ab7751) and MAP2 (rabbit polyclonal to microtubule-associated protein 2, Cell Signaling Technology #4542). Secondary antibodies were: anti-rabbit IgG-Cy3 (Sigma, #C2306) and anti-mouse IgG-DyLight[®] 549 (Vector, #DI-2549). The cells were analyzed on the Zeiss AXIO Observer.Z1 inverted microscope equipped with Hamamatsu Digital Camera C10600 Orca R². Images were acquired using AxioVision Rel. 4.7 program. The objective lenses were Zeiss EC Plan-NEOFLUAR 10X/0,3 Ph1 (420341-9911) and Zeiss LD Plan-NEOFLUAR 20X/0,4 Ph2 Korr (∞/0-1,5). The images of individual neurons were saved as .tif files which were opened in NeuroLucida[®] software for neuron reconstruction and morphometry. The individual neurons were traced and analyzed in NeuroExplorer with results presented in spreadsheet format and exported to Microsoft Excel[®]. We analyzed 10-14 images for each group (total 70 images). The statistical significance was measured using two tailed t-test in MS-Exec 2007.

Lipid extraction, separation, HPLC-APCI-MS-MS analyses, *preparation of 7-DHC-derived oxysterols and DHCEO*, were done as previously described^{7, 8}.

RESULTS

Cholesterol decrease and 7-DHC accumulation vary across brain regions in Dhcr7-KO mice

Cholesterol and 7-DHC levels were analyzed across the neocortex, hippocampus, midbrain/brainstem, and cerebellum (Figure 1). In the WT animals we found a relatively uniform cholesterol levels across the four tested brain regions, ranging from 21.0 µg/mg protein (n=3) in hippocampus to 35.2 µg/mg protein (n=3) in the midbrain. In *Dhcr7-KO* brain, cholesterol concentrations showed a large reduction relative to corresponding controls, and ranged from 4.1 µg/mg protein in midbrain (n=5) to 6.9 µg/mg protein in hippocampus (n=5) which suggests that cholesterol was reduced ~ 3 times in the hippocampus and ~ 9 times in the midbrain in *Dhcr7-KO* mice. While 7-DHC was not detectable in WT brain tissue, 7-DHC levels varied from 10.5 µg/mg protein in cerebellum (n=5) to 36.6 µg/mg in the midbrain (n=5) in the *Dhcr7-KO* mice. Thus, while in the hippocampus and cerebellum of *Dhcr7-KO* mice 7-DHC levels equaled to about double of total cholesterol levels seen in the WT, in the cortex and midbrain 7-DHC levels were roughly equivalent to cholesterol levels observed in the WT mice (Figure 1). This suggests that the consequences of 7-DHC

accumulation (and/or cholesterol reduction) would be the most pronounced in the cortex and midbrain regions.

DHCEO formation does not follow 7-DHC accumulation in specific brain regions

7-DHC is highly oxidizable and the autoxidation of 7-DHC generates over a dozen specific oxysterols, including DHCEO^{6, 7}. Importantly, DHCEO is also the major oxysterol identified in the human fibroblasts derived from SLOS patients and in the whole brain of Dhcr7-KO mice⁶. This led us to the hypothesis that 7-DHC levels would predict DHCEO levels across the investigated brain regions. Surprisingly, this was not always the case: the highest amount of DHCEO was found in the neocortex (17.2 ng/mg protein, n=5) and midbrain (21.7 ng/mg protein, n=5) regions, while the hippocampus and cerebellum reported considerably less accumulation of DHCEO (4.8 ng/mg protein, n=5 and 9.8 ng/mg protein, n=5, respectively). Furthermore, the ratio of DHCEO to 7-DHC varied across the four brain regions, and it ranged from 0.93 (cerebellum) to 0.39 (hippocampus) (Figure 2). This suggests that conversion of 7-DHC to oxysterols is a regulated process, and that oxysterol levels are region-specific, and a result of either different rate of 7-DHC derived oxysterol formation or different clearance rates of 7-DHC derived oxysterols across the tissues. Therefore, assuming that 7-DHC derived oxysterols have an ability of interfering with neuronal development/function, one would predict that the consequences of oxysterol accumulation would be the most prominent in the cortex and midbrain, as this was already predicted based on cholesterol and 7-DHC levels.

Cytotoxicity of 7-DHC-derived oxysterols is an order of magnitude higher in cortical neurons than glia

Oxidation of 7-DHC generates a number of oxysterols, including DHCEO⁷. To test if these oxysterols are detrimental to cell function, we next established the sensitivity of cortical neurons and astrocytes to a 7-DHC-derived oxysterol mixture. Our results revealed that oxysterol concentrations that have been found in the brain of SLOS mice⁷ show approximately 10-fold more cytotoxicity to neocortical neurons than astrocytes (Figure 3). At 500 nM concentration, the 7-DHC-derived oxysterol mixture did not affect viability of astrocytes, yet it led to a 30% reduction of viability of cortical neurons (p=0.05; n=3). These data suggest that 7-DHC derived oxysterols, even at low concentrations, have a toxic effect on neurons, and are capable of altering normal neural development.

Exposure to DHCEO accelerates *in vitro* differentiation of neuronal processes

Since we previously showed that the 7-DHC derived oxysterol DHCEO is moderately toxic in Neuro2A cells⁸, we wanted to test if DHCEO exposure can contribute to the neurotoxic effects of the 7-DHC derived oxysterol mixture on primary cortical neurons. While DHCEO is the major 7-DHC-derived oxysterol identified in the Dhcr7-KO mouse brain⁷, it is a very minor product in the 7-DHC-derived oxysterol mixture produced in the test tube⁶. E18 cortical neurons were cultured for 3 days, followed by a single exposure of 5 μ M DHCEO (a level that is found in the brain of SLOS mice⁷), and assayed after 48 hours. Exposure of cortical neurons to DHCEO did not affect cell viability (data not shown), however, it had a profound effect on cellular morphology. Control neurons were not fully differentiated, had only a few processes, and supported multiple growth cones (Figure 4A). In contrast, neurons treated with DHCEO showed distinct morphology with very long and brightly stained processes without growth cones, having an appearance of fully differentiated neurons (Figure 4A). Staining with both Tu20 and MAP2 (both of which are widely used to identify neurons in culture⁹) showed consistent findings (data not shown). Based on the method of Kriegstein and Dichter¹⁰ we used specific morphological characteristics to identify three types of neurons in our tissue culture: pyramidal-like, multipolar, and fusiform (Figure 4B). Examples of camera lucida tracings of individual neurons are shown in Figure 5A. We

compared the total arborization of these three morphological classes of neurons between DHCEO-treated and control cultures (Figure 5B). Quantification revealed that all three classes of neurons reported a statistically significant and comparable increase of total process length. To better understand the branching characteristics of control and DHCEO-treated neurons we did Sholl analysis¹¹ (Figure 5C). The quantification of the length of dendrites at different intersections of concentric circles centered at the cell body shows that DHCEO-treated neurons have higher density of neuronal processes and the arborization is present at greater distance away from the cell body.

The morphological changes, in the absence of effect on neuronal viability, reveal two intriguing conclusions. First, that toxicity of the 7-DHC oxysterol mixture in cortical neurons is mediated by either the cumulative effect of the total oxysterol mixture, or a specific oxysterol fraction (but not DHCEO) that remains to be identified. For example, major components of the 7-DHC-derived oxysterol mixture including oxysterols 2 α , 2 β , and 3⁸ were shown to be the most toxic compounds to Neuro2a cells, probably due to the endoperoxide moiety within the molecular structures. The same set of compounds could contribute to the overall toxicity of the oxysterol mixture to cortical neurons. Second, it suggests that DHCEO exposure accelerates neuronal maturation, potentially altering the normal developmental trajectory of the brain.

DISCUSSION

The current studies revealed four critical findings concerning the pathophysiology by which *Dhcr7* mutation and 7-DHC accumulation lead to altered brain development and function in SLOS: 1) In a mouse SLOS model, 7-DHC and its metabolite DHCEO, show specific accumulation across the brain regions, suggesting that the most pronounced pathophysiological events occur in the midbrain and neocortical regions; 2) the DHCEO and 7-DHC ratio is not constant across the brain regions, and thus oxysterol formation is likely to be a process that is actively and differentially regulated across the various brain regions; 3) 7-DHC derived oxysterols, at concentrations observed in brain tissues of *Dhcr7*-KO mouse, are strongly neurotoxic, while the same concentrations have little effect on glial cell viability; 4) DHCEO cannot fully account for the cytotoxicity of 7-DHC derived oxysterols, but it strongly accelerates differentiation and neurite outgrowth in neocortical neuronal cultures.

The different production/turnover of cholesterol in the normal brain, together with different 7-DHC and 7-DHC derived oxysterol distribution across the brain regions of the SLOS mouse model has several important implications. First, it appears that the normal accumulation of cholesterol is vastly different between the various brain regions, and potentially across the various subpopulations of cells. This view is strongly supported by previous *in situ* hybridization reports against *Dhcr7*, which revealed both a regional and cell-type specific pattern of *Dhcr7* mRNA localization². Second, the variable ratio of DHCEO/7-DHC across the brain regions of the SLOS mouse model strongly suggests that the generation of 7-DHC derived oxysterols is, at least in part, a regulated process. These differences could be explained by multiple mechanisms such as different formation rates of oxysterols, different antioxidant capacity for free radical oxidation or differential clearance mechanisms in the various cell types. The presumed mechanism for oxysterol formation is a free radical chain reaction that can be inhibited by antioxidants⁷. Further research is needed to determine if there might be other, currently unknown mechanisms by which oxysterols are formed in the brain tissue. The detrimental effects of 7-DHC derived oxysterols on the neurons suggest that identifying the intracellular mediators of oxysterol formation is an important direction of future research, as these molecules might hold a key to therapeutic interventions. At this time it remains unknown if the *in vivo* neurotoxicity is best explained

by absolute tissue 7-DHC levels, the ratio between oxysterols and 7-DHC and, overall oxysterol levels, or specific oxysterol concentrations.

While our results clearly indicate that 7-DHC derived oxysterol mixture is neurotoxic, they also suggest that DHCEO, at the concentration observed in brain tissues of *Dhcr7*-KO mouse, cannot account for a majority of the observed toxicity. This suggests that the various 7-DHC derived oxysterols might represent cumulative, yet distinct risks to the central nervous system: DHCEO appears to accelerate differentiation, disrupting the normal neurodevelopmental process, while other, currently unidentified oxysterols mediate neurotoxicity⁶. This is potentially a converging, two-hit insult to the developing nervous system, putatively leading to altered neuronal structure and connectivity¹², and ultimately might give rise to the symptoms of SLOS. Support to this view comes from both studies in SLOS patients and investigations of SLOS mouse models: patients with SLOS show frontal lobe hypoplasia, cortical migration defect, and abnormalities of median line structures corresponding to corpus callosum^{13, 14}, and SLOS mice show increased arborization of neuronal dendritic tree and reduced brain volume^{15, 16}.

In summary, we believe that in SLOS the accumulation of 7-DHC leads to a brain region-specific formation of 7-DHC-derived oxysterols. This mixture has two main effects in the brain - affects expression of many transcripts¹⁷ (also previously demonstrated in our *Dhcr7*-KO cell culture model⁸), and it leads to premature neuronal differentiation, most likely due to DHCEO formation in the brain tissue. Identifying the intracellular mechanisms that regulate tissue-specific oxysterol levels might give us valuable clues on how to reduce 7-DHC-derived oxysterol formation, enhance the resilience of cells, or increase clearance of these toxic metabolites, and thus should be one of the critical avenues of further research. Furthermore, identifying the individual fraction or fractions of 7-DHC metabolites that mediate neurotoxicity is of great interest for fully understanding the pathophysiological events in the brain of SLOS patients. Finally, our results also imply that reducing oxidative stress is the right strategy for treatment of SLOS.

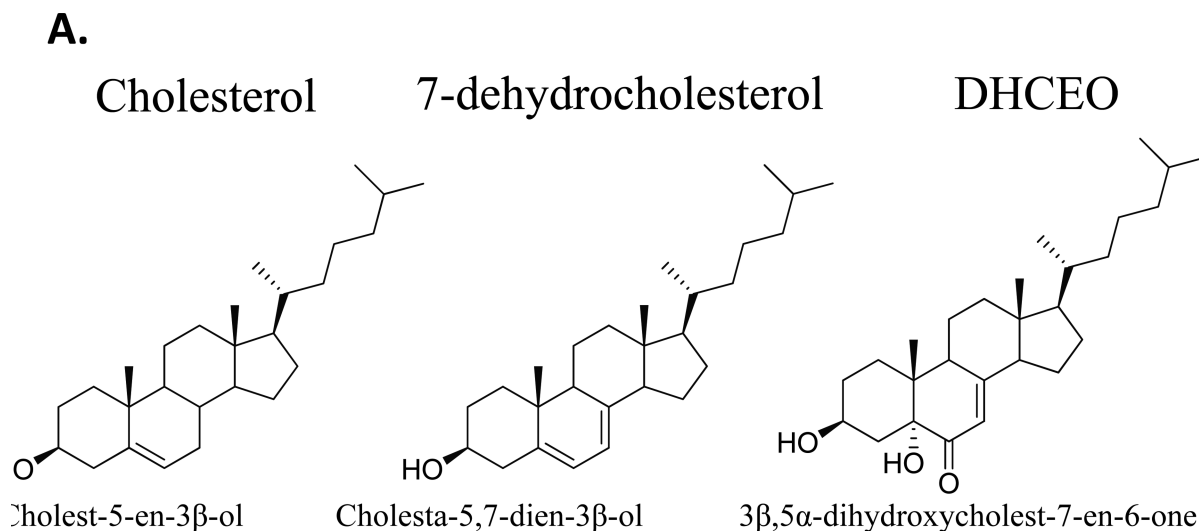
Acknowledgments

The National Institutes of Health (1R01 MH079299 and 2R01MH067234 to KM; NIEHS ES0016931 to ABB; NICHD HD064727 to NP) supported this work. Z.K appreciates support from the Vanderbilt Kennedy Center for Research on Human Development. The authors thank Dr. Georges Barnes for the use of NeuroLucida system.

REFERENCES

1. Dietschy JM, Turley SD. Cholesterol metabolism in the brain. *Curr Opin Lipidol*. 2001; 12(2):105–112. [PubMed: 11264981]
2. Korade Z, Mi Z, Portugal C, Schor NF. Expression and p75 neurotrophin receptor dependence of cholesterol synthetic enzymes in adult mouse brain. *Neurobiol Aging*. 2007; 28(10):1522–1531. [PubMed: 16887237]
3. Irons M, Elias ER, Salen G, Tint GS, Batta AK. Defective cholesterol biosynthesis in Smith-Lemli-Opitz syndrome. *Lancet*. 1993; 341(8857):1414. [PubMed: 7684480]
4. Tierney E, Nwokoro NA, Kelley RI. Behavioral phenotype of RSH/Smith-Lemli-Opitz syndrome. *Ment Retard Dev Disabil Res Rev*. 2000; 6(2):131–134. [PubMed: 10899806]
5. Xu L, Davis TA, Porter NA. Rate constants for peroxidation of polyunsaturated fatty acids and sterols in solution and in liposomes. *J Am Chem Soc*. 2009; 131(36):13037–13044. [PubMed: 19705847]
6. Xu L, Korade Z, Porter NA. Oxysterols from free radical chain oxidation of 7-dehydrocholesterol: product and mechanistic studies. *J Am Chem Soc*. 2010; 132(7):2222–2232. [PubMed: 20121089]

7. Xu L, Korade Z, Rosado DA Jr, Liu W, Lamberson CR, Porter NA. An oxysterol biomarker for 7-dehydrocholesterol oxidation in cell/mouse models for Smith-Lemli-Opitz syndrome. *J Lipid Res.* 2011; 52(6):1222–1233. [PubMed: 21402677]
8. Korade Z, Xu L, Shelton R, Porter NA. Biological activities of 7-dehydrocholesterol-derived oxysterols: implications for Smith-Lemli-Opitz syndrome. *J Lipid Res.* 2011; 51(11):3259–3269. [PubMed: 20702862]
9. Banker, G.; Goslin, editors. *Culturing nerve cells.* Cambridge: MA: 1991.
10. Kriegstein AR, Dichter MA. Morphological classification of rat cortical neurons in cell culture. *J Neurosci.* 1983; 3(8):1634–1647. [PubMed: 6875660]
11. Sholl DA. Dendritic organization in the neurons of the visual and motor cortices of the cat. *J Anat.* 1953; 87(4):387–406. [PubMed: 13117757]
12. Korade Z, Mirmics K. Gene expression: The autism disconnect. *Nature.* 2011; 474(7351):294–295. [PubMed: 21677744]
13. Caruso PA, Poussaint TY, Tzika AA, Zurakowski D, Astrakas LG, Elias ER, et al. MRI and 1H MRS findings in Smith-Lemli-Opitz syndrome. *Neuroradiology.* 2004; 46(1):3–14. [PubMed: 14605787]
14. Mueller C, Patel S, Irons M, Antshel K, Salen G, Tint GS, et al. Normal cognition and behavior in a Smith-Lemli-Opitz syndrome patient who presented with Hirschsprung disease. *Am J Med Genet A.* 2003; 123A(1):100–106. [PubMed: 14556255]
15. Jiang XS, Backlund PS, Wassif CA, Yergey AL, Porter FD. Quantitative proteomics analysis of inborn errors of cholesterol synthesis: identification of altered metabolic pathways in DHCR7 and SC5D deficiency. *Mol Cell Proteomics.* 2011; 9(7):1461–1475. [PubMed: 20305089]
16. Jiang XS, Wassif CA, Backlund PS, Song L, Holtzclaw LA, Li Z, et al. Activation of Rho GTPases in Smith-Lemli-Opitz syndrome: pathophysiological and clinical implications. *Hum Mol Genet.* 2011; 19(7):1347–1357. [PubMed: 20067919]
17. Waage-Baudet H, Dunty WC Jr, Dehart DB, Hiller S, Sulik KK. Immunohistochemical and microarray analyses of a mouse model for the smith-lemli-opitz syndrome. *Dev Neurosci.* 2005; 27(6):378–396. [PubMed: 16280635]
18. Wassif CA, Zhu P, Kratz L, Krakowiak PA, Battaile KP, Weight FF, et al. Biochemical, phenotypic and neurophysiological characterization of a genetic mouse model of RSH/Smith-Lemli-Opitz syndrome. *Hum Mol Genet.* 2001; 10(6):555–564. [PubMed: 11230174]
19. Fitzky BU, Moebius FF, Asaoka H, Waage-Baudet H, Xu L, Xu G, et al. 7-Dehydrocholesterol-dependent proteolysis of HMG-CoA reductase suppresses sterol biosynthesis in a mouse model of Smith-Lemli-Opitz/RSH syndrome. *The Journal of clinical investigation.* 2001; 108(6):905–915. [PubMed: 11560960]

**B.**

Brain Region	Genotype	Cholesterol $\mu\text{g}/\text{mg}$ protein	7DHC $\mu\text{g}/\text{mg}$ protein	DHCEO ng/mg protein
Cortex	WT	32.0 \pm 2.1	< 0.2	not detected
Cortex	KO	4.8 \pm 0.7	22.4 \pm 3.3	17.2 \pm 1.8
Midbrain	WT	35.2 \pm 2.7	< 0.2	not detected
Midbrain	KO	4.1 \pm 0.7	36.6 \pm 13.0	21.7 \pm 2.0
Hippocampus	WT	21.0 \pm 1.1	< 0.2	not detected
Hippocampus	KO	6.9 \pm 1.7	12.3 \pm 2.6	4.8 \pm 0.9
Cerebellum	WT	21.7 \pm 0.4	< 0.2	not detected
Cerebellum	KO	5.8 \pm 0.8	10.5 \pm 2.2	9.8 \pm 1.9

Figure 1. Structure and expression of cholesterol, 7-dehydrocholesterol and DHCEO in WT and *Dhcr7*-KO mouse brain tissue

A) Chemical structure of cholesterol, immediate cholesterol precursor 7-DHC, and DHCEO, which is derived from 7-DHC by oxidation. **B)** Expression of cholesterol, 7-DHC, and DHCEO levels in cortex, midbrain, hippocampus and cerebellum in E20 mouse brain tissue. 7-DHC levels < 0.2 $\mu\text{g}/\text{mg}$ in WT are consistent with previously published measurements of 7-DHC in the mouse brain tissue^{18, 19}. DHCEO level in WT tissue was below the limit of detection for LC/MS (less than 2 ng). Note the high, but variable levels of 7-DHC and DHCEO across the various brain regions of the *Dhcr7*-KO mice.

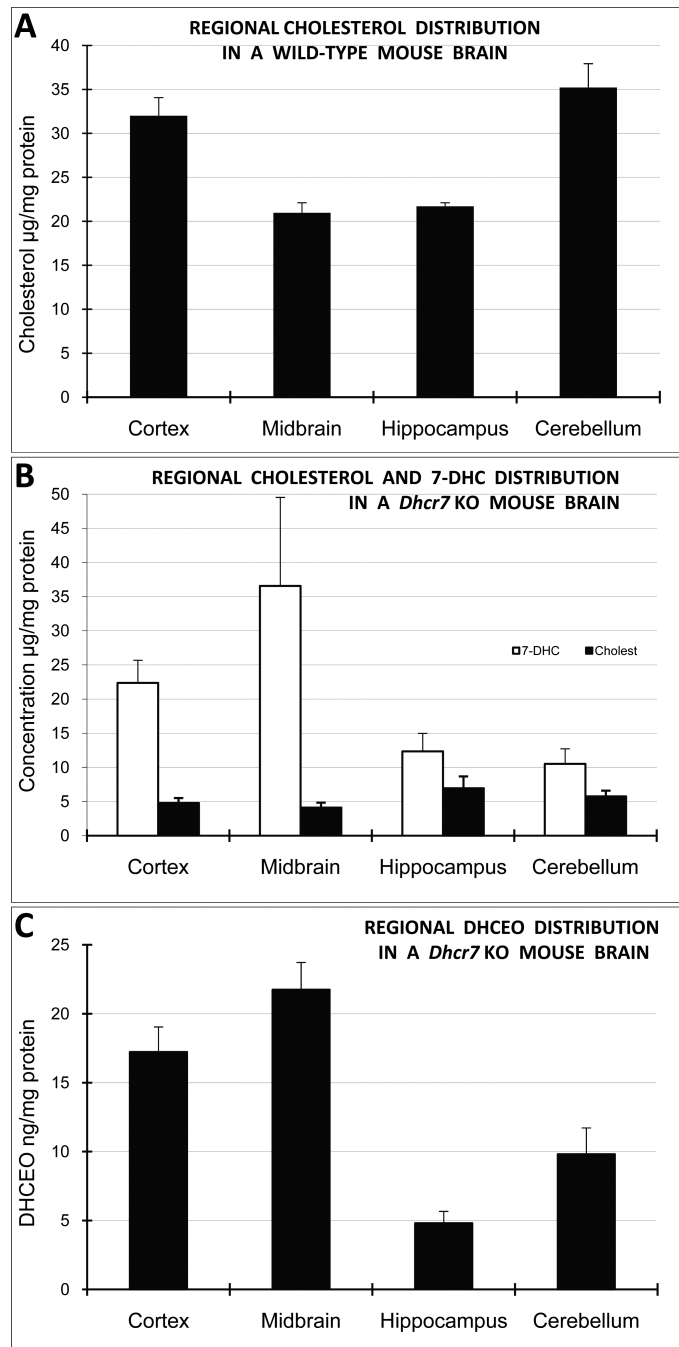


Figure 2. 7-DHC and DHCEO accumulation vary across brain regions in *Dchr7*-KO mice
 A) Normalized cholesterol levels are highest in the cortex and cerebellum in the WT mouse brain. B) The highest amount of 7-DHC is found in midbrain and cortex in *Dchr7*-KO mice, with strongly diminished and uniform levels of cholesterol across all the brain regions. C) The highest levels of DHCEO are formed in cortex and midbrain. Note that cholesterol and/or 7-DHC are not predictive of DHCEO levels across the brain regions.

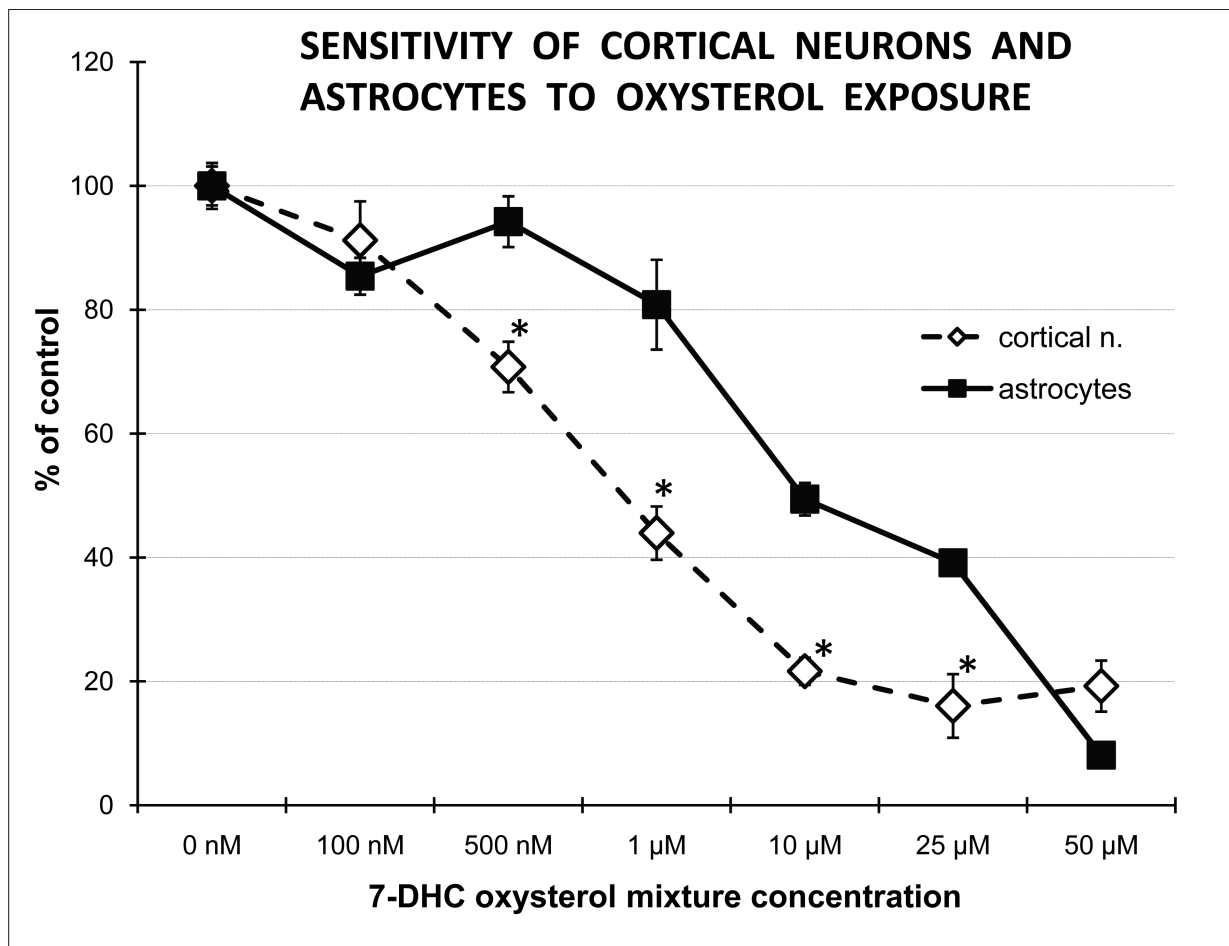


Figure 3. 7-DHC-derived oxysterols are highly neurotoxic

X-axis denotes concentrations of oxysterols while y-axis shows the percentage of live cells compared to untreated controls. Primary cortical neurons and astrocytes were treated with different concentrations of 7-DHC oxysterol mixture for 72 hrs. Cell survival was measured using CellTiterProliferation Assay (Promega). Note that oxysterols, in concentrations comparable to those found in the brain of SLOS mice⁷, show approximately 10-fold higher cytotoxicity to neocortical neurons than astrocytes.

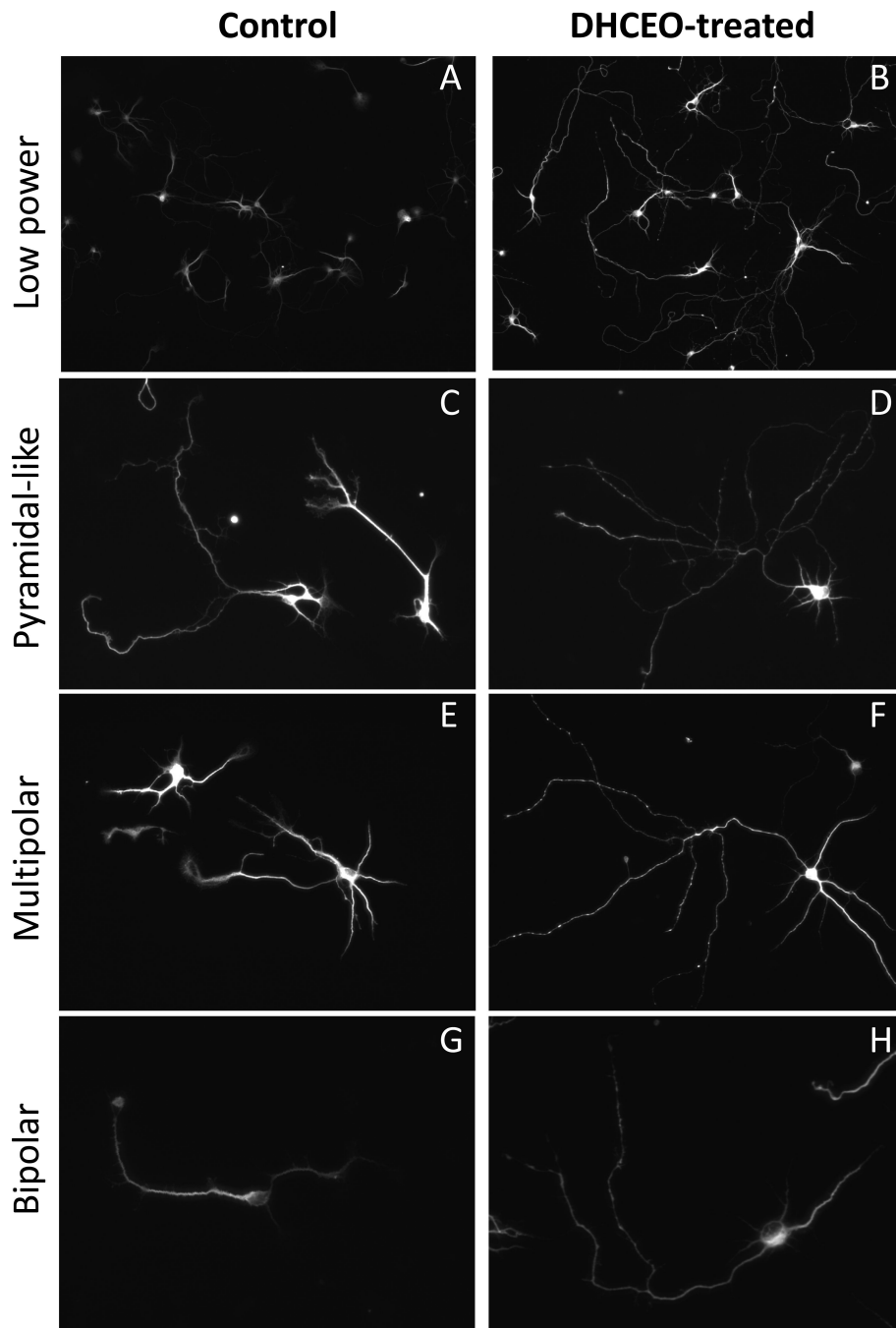


Figure 4. Differentiation of neuronal processes *in vitro* is accelerated in the presence of DHCEO Primary cortical neurons were grown for 3 days and then treated with 7-DHC-derived oxysterol DHCEO for 48 hrs. **A-B)** Example of control and DHCEO-treated cultures stained with MAP2 antibody (cal bar = 50 μm). Unaltered images were acquired at the same exposure times showing more pronounced intensity of staining in DHCEO-treated cultures, suggesting relative immaturity of control cultures compared to DHCEO-treated ones. **C-H)** Examples of different neuronal types in cultures exposed to sham- and DHCEO treatment (cal bar = 100 μm). Note that in all figures DHCEO-treated neurons show more extensive neuronal arborization.

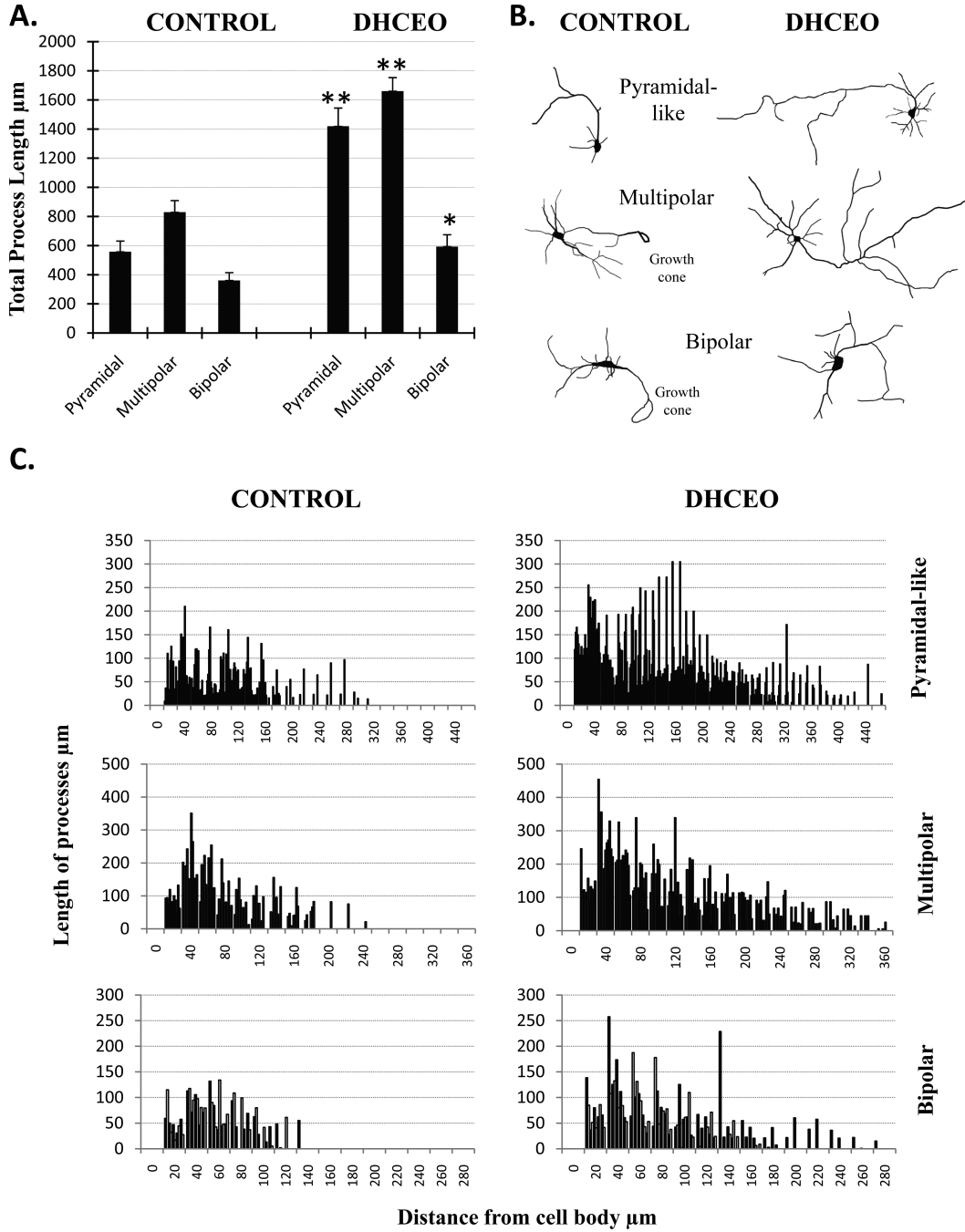


Figure 5. DHCEO-treated neurons show a statistically significant increase in process arborization across the various morphological classes of neurons
A) Pyramidal-like, multipolar and bipolar neurons all report a statistically significant increase in total process length after 72 hours of DHCEO exposure (10-14 neurons per group, * $p < 0.01$; ** $p < 0.001$). **B)** Typical examples of neuroLucida-traced cortical neurons exposed to sham or DHCEO treatment. **C)** Graphical representation of process arborization as determined by Sholl Analysis, performed on neuroLucida-traced neurons. Each bar represents a different neuron.